Supplemental Data
Cell, Volume *133*

Identification of Positionally Distinct Astrocyte Subtypes whose Identities Are Specified by a Homeodomain Code

Christian Hochstim, Benjamin Deneen, Agnès Lukaszewicz, Qiao Zhou, and David J. Anderson

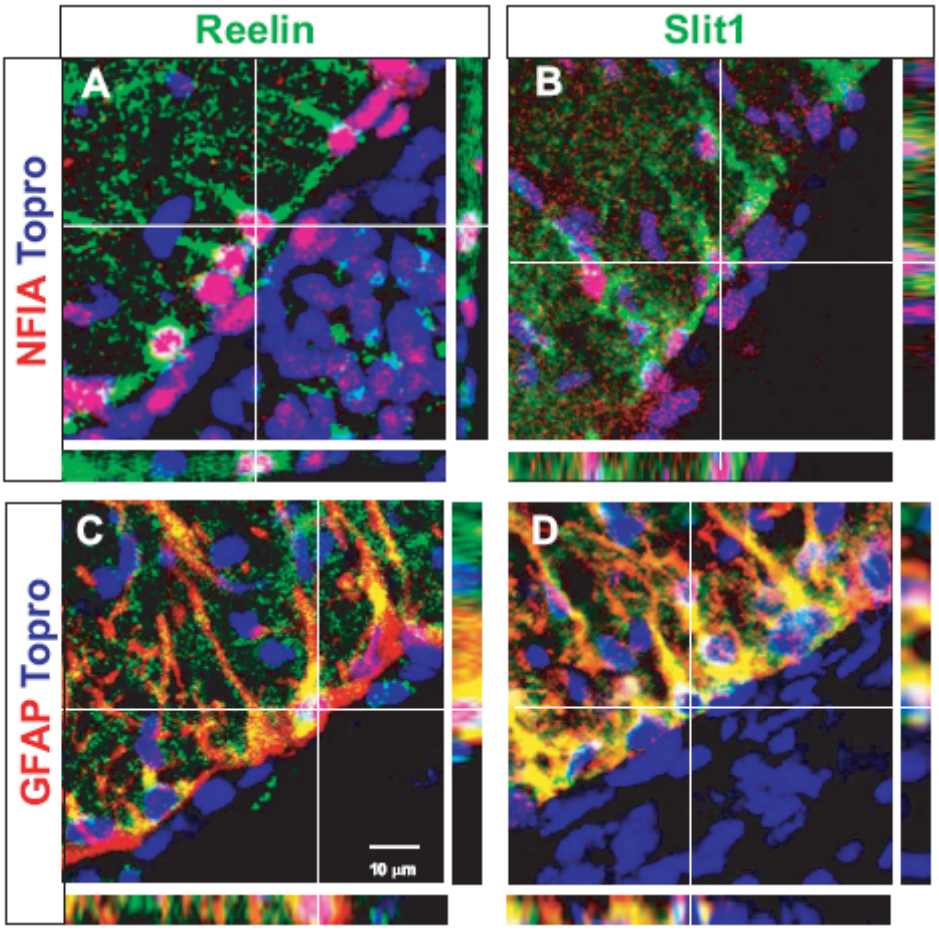

Figure S1. Z-series analysis of Reelin and Slit1 expression in relationship to astrocyte markers in the WM at E18.5.

Double-labeling was performed for Reelin (A, C) and Slit1-GFP (B, D) and either NFIA (A, B) or GFAP (C, D). Note that the NFIA$^+$ nuclei indicated by the cross-hairs in (A) and (B) are surrounded by Reelin$^+$ (A) or Slit1$^+$ (B) labeling. Z-series analysis is shown below and to the right of each image. In (C, D) note that Topro$^+$ nuclei (included as a counter-stain) are surrounded by GFAP$^+$, Reelin$^+$ (C) or GFAP$^+$, Slit1$^+$ (D) labeling. Scale bars, 10 µm.

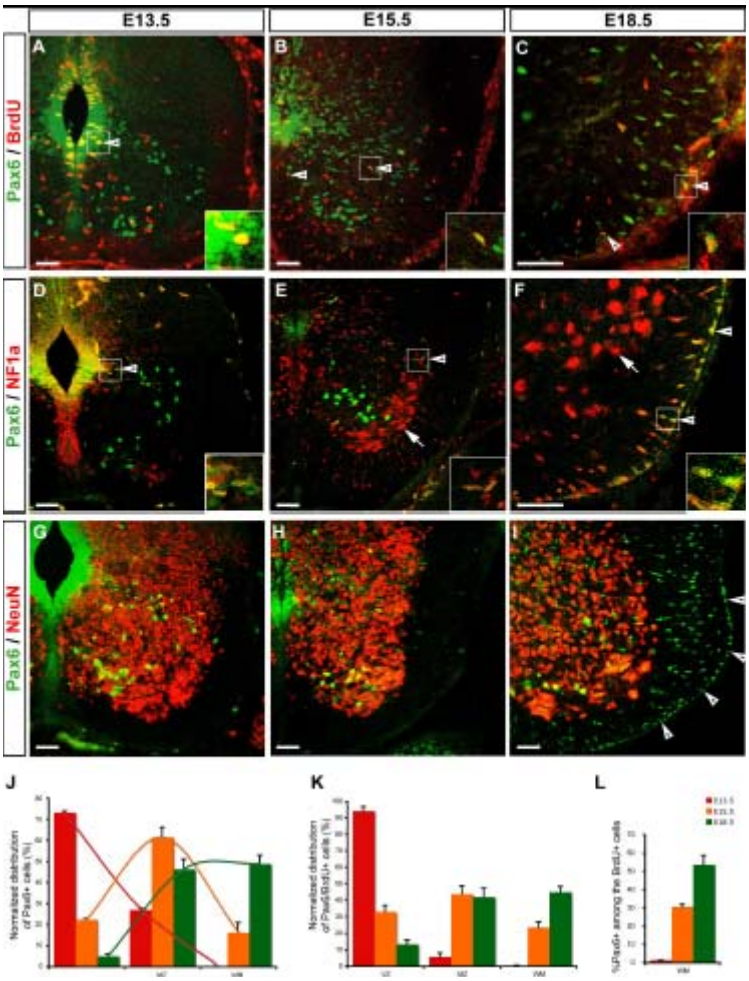

Figure S2. Pulse-chase analysis of Pax6$^+$ cells in the E13.5 VZ.

Pregnant mice were pulsed with BrdU (50 µg/g body weight) at E13.5, and analyzed at the indicated times; "E13.5" denotes 2 hrs after the BrdU pulse. By E13.5, neurons are no longer being generated from the ventral region of the VZ where Pax6$^+$ cells are located. (A-I) sections of spinal cord double-labeled for Pax6 (green) and the indicated markers (red) at different stages. Insets (A-F) represent higher-magnification views of the cells labeled by the arrowheads. (J) Distribution of Pax6$^+$ cells between the VZ, mantle zone (MZ) and WM at E13.5 (red), E15.5 (orange) and E18.5 (green), normalized to 100%. At 13.5, the majority of Pax6$^+$ cells are located in the VZ; at E15.5 the majority are located in the MZ, and at E18.5 they are equally distributed between the MZ and WM. Note that, at E15.5, at least some of the Pax6$^+$ cells in the MZ are NFIA$^+$ (E, arrowhead). Arrows in (E, F) indicate expression of NFIA in motoneurons (Deneen et al., 2006), which are identifiable by their size and characteristic location. (K) Distribution of Pax6$^+$, BrdU$^+$ cells as in (J), normalized to 100%. Note the progressive shift in the distribution from the VZ→MZ→WM, from E13.5→E15.5→E18.5. The absolute labeling index of Pax6$^+$ cells in the VZ at E13.5 was 16.1%; conversely, ~85% of BrdU$^+$ cells were Pax6$^+$. (L) Percentage of BrdU$^+$ cells in the WM expressing Pax6. Note that by E18.5, >50% of all BrdU$^+$ cells in the WM are Pax6$^+$. Scale bars in (A-I), 50 µm. Data represent mean±S.E.M. from 2 independent BrdU injection experiments, with 2-3 embryos analyzed per time point per experiment, except for E15.5 (n=1 injection, 5 embryos analyzed).

Quantitative analysis: The increased proportion of $Pax6^+$ cells in the WM between E15.5 and E18.5 (J) could reflect either the induction of expression in resident cells, or the migration of $Pax6^+$ cells from the MZ. We asked whether the increase in $Pax6^+$ cells in the WM could be quantitatively accounted for by the actual loss of cells from the MZ, assuming that the observed loss reflects the actual loss, offset by the gain of cells migrating from the VZ→MZ during the same interval. The net gain in WM $Pax6^+$ cells between E15.5 and E18.5 = (48.8% - 16.2%) = 32.6% of the total $Pax6^+$ population. The observed loss of $Pax6^+$ cells from the MZ between E15.5 and E18.5 is (61.4%-46.2%) = 15.2%. Assuming that this observed loss is compensated by a gain of $Pax6^+$ cells migrating from the VZ, the extent of this gain should be equal to the decrease in $Pax6^+$ cells in the VZ between E15.5 and E18.5 = (22.8%-5%) = 17.8%. Therefore the actual loss of $Pax6^+$ cells from the MZ would be the observed loss + 17.8% (17.8%+15.2%) = 33%. This number is remarkably close to the observed increase in $Pax6^+$ cells in the WM between E15.5 and E18.5 (32.6%). Similarly, the proportion of $Pax6^+$ cells in the MZ increases from 26.9% to 61.4% between E13.5 and E15.5, a net gain of 34.5%. This is very close to the number calculated by assuming that the net increase in MZ $Pax6^+$ cells reflects the addition of cells lost from the VZ (73.1-22.4=50.7%) minus the number added to the WM (16.2%), i.e., 34.5%. While these similarities could be coincidental, the observation that cells pulse-labeled with BrdU in the VZ at E13.5 can be chased into the WM at E18.5, and that over half of these WM $BrdU^+$ cells are $Pax6^+$, suggests that the most parsimonious interpretation of the data is that at least some $Pax6^+$ cells in the VZ at E13.5 are indeed precursors of $Pax6^+$ WMAs at E18.5.

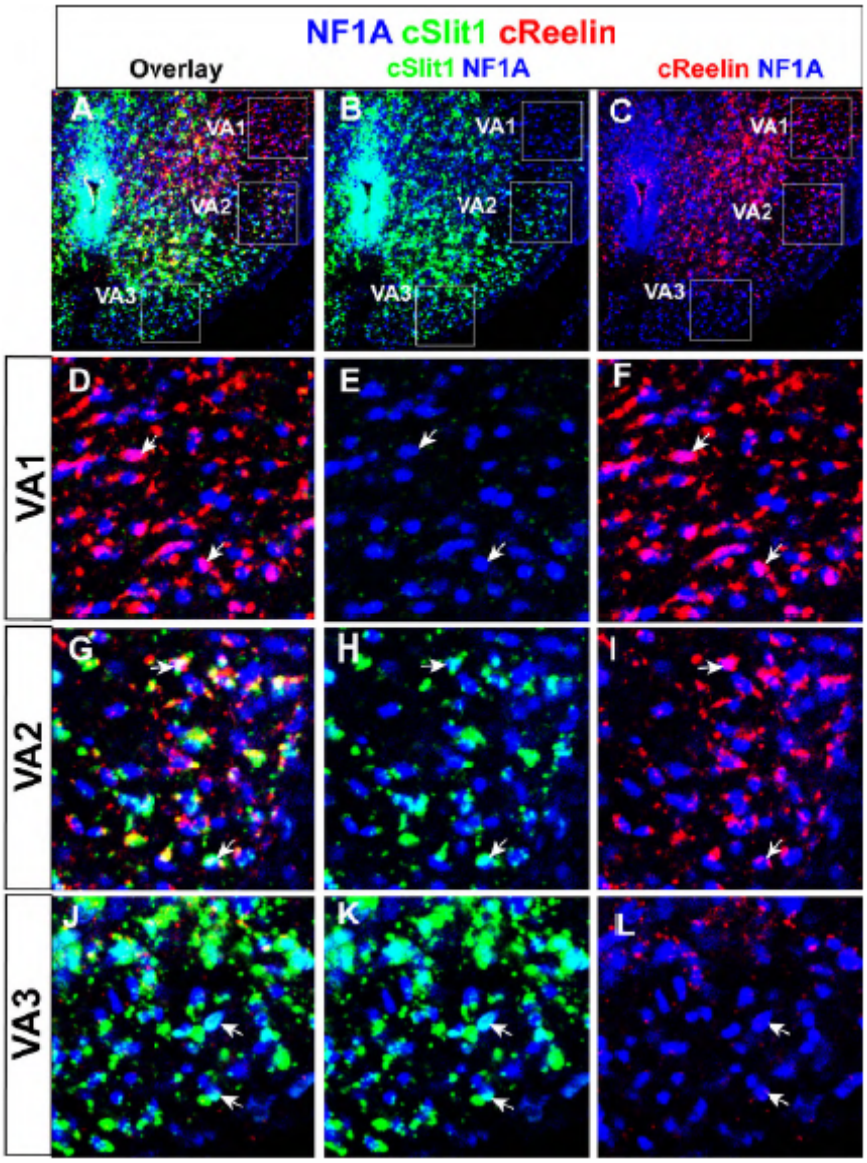

Figure S3. Reelin and Slit1 mark astrocvte subpopulations in chick spinal cord

Representative section from the ventro-lateral quadrant of an E12 chick embryos triple-labeled with antibody to NF1A and fluorescent in situ hybridization for cSlit1 and cReelin mRNAs. (A-C) Low magnification views of the same section with cSlit1 (B) and cReelin (C) shown as separate channels in comparison to NF1A. (D-L) Higher magnification views of the boxed areas shown in (A-C). As in the mouse, VA1 astrocytes (D-F) express cReelin (F) but not cSlit1 (E), VA2 astrocytes (G-I) express both cSlit1 (H) and cReelin (I), and VA3 astrocytes express cSlit1 (K) but not Reelin (L).

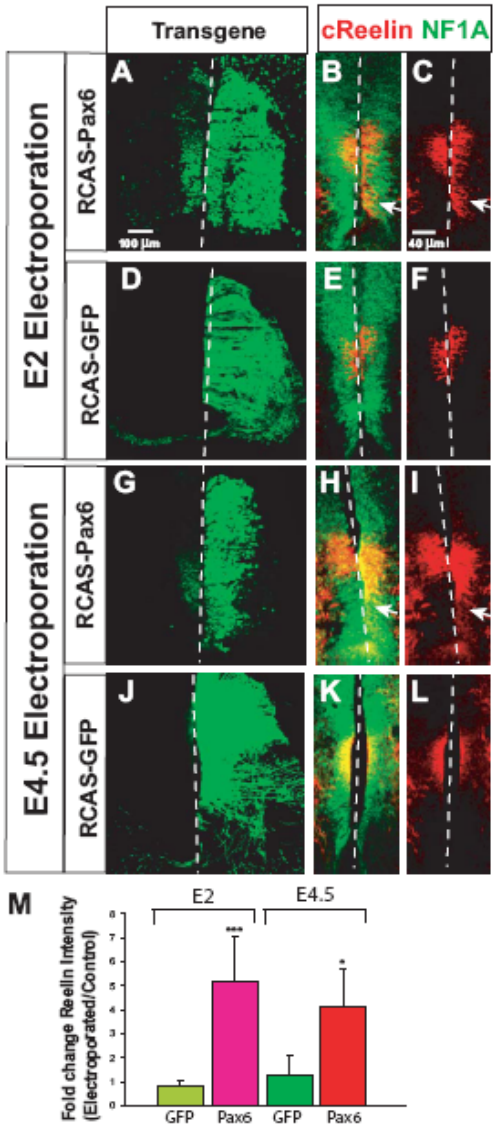

Figure S4. Mis-expression of Pax6 at both E2 and E4.5 causes a ventral expansion of Reelin mRNA expression within the VZ.

Chick embryonic spinal cord was electroporated at E2 and analyzed at E5 (A-F; M "E2"), or electroporated at E4.5 and analyzed at E5.5 (G-L, M "E4.5"). "Transgene" indicates expression of Pax6 or GFP. the electroporated side of the spinal cord is to the right of the dashed vertical line (which delineates the ventricle) in all panels. Mis-expression of Pax6 at either E2 or E4.5 causes a ventral expansion of Reelin in the VZ (C, I; arrows). The expression of NF1A in these VZ cells marks their specification for a glial fate (B, H; arrows). (M) Quantification based on integrated pixel intensity. (***, $p<.001$; *, $p<.01$).

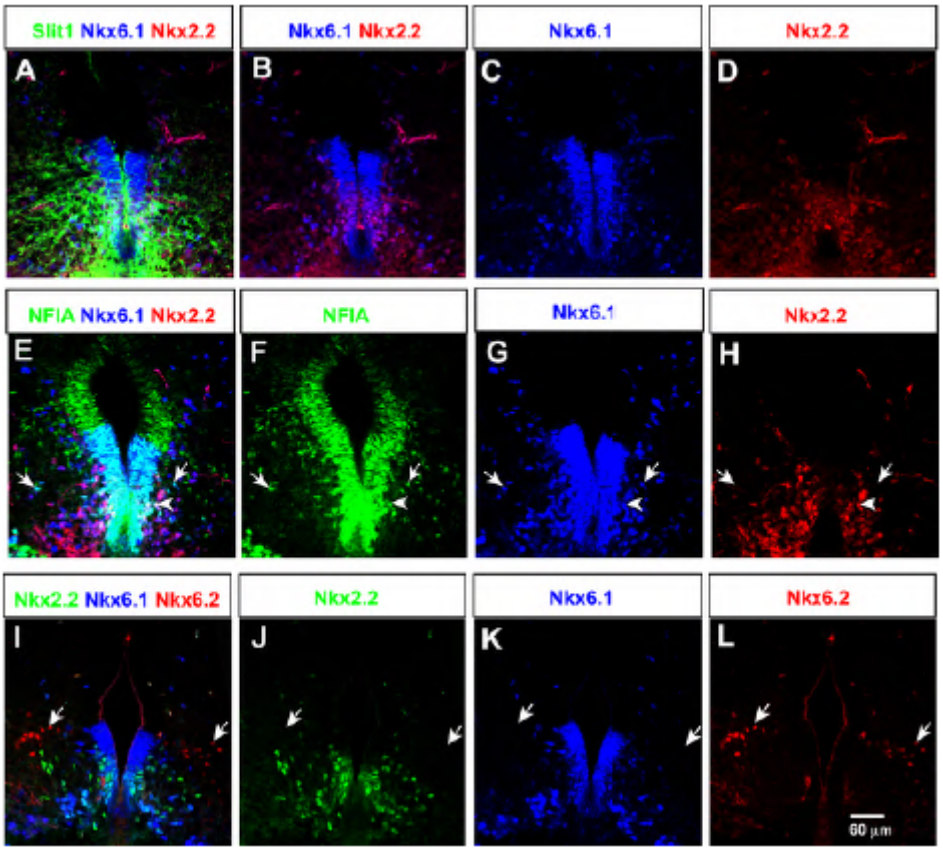

Figure S5. Expression of Nkx2.2 and Nkx6.2 during early gliogenesis

(A-D) Sections through the ventral ventricular zone of mouse E13.5 *Slit1-GFP/+* embryos, triple-labeled with antibodies to GFP, Nkx6.1 and Nkx2.2. Note that Nkx2.2 is expressed in the ventral VZ, in a region that overlaps with Nkx6.1 (B) and Slit1 (A). Some Nkx6.1$^+$ Nkx2.2$^+$ cells can be seen to be apparently migrating away from the VZ. (E-F) Triple-labeling for NF1A, Nkx6.1 and Nkx2.2. Nkx2.2$^+$ cells are NF1A$^+$ within the VZ, and a few double-positive cells can be seen apparently delaminating from the ventricular zone; these cells are also Nkx6.1$^+$ (arrowhead). However most NF1A$^+$, Nkx6.1$^+$ astrocyte precursors that appear to be migrating into the gray matter are Nkx2.2$^-$ (arrows). (I-J) at this stage, Nkx6.2 (red staining) is not expressed within the VZ, dorsal to the Nkx6.1 domain (Briscoe et al., 2000; Vallstedt et al., 2001), but is only detected in a subset of interneurons (I, L).

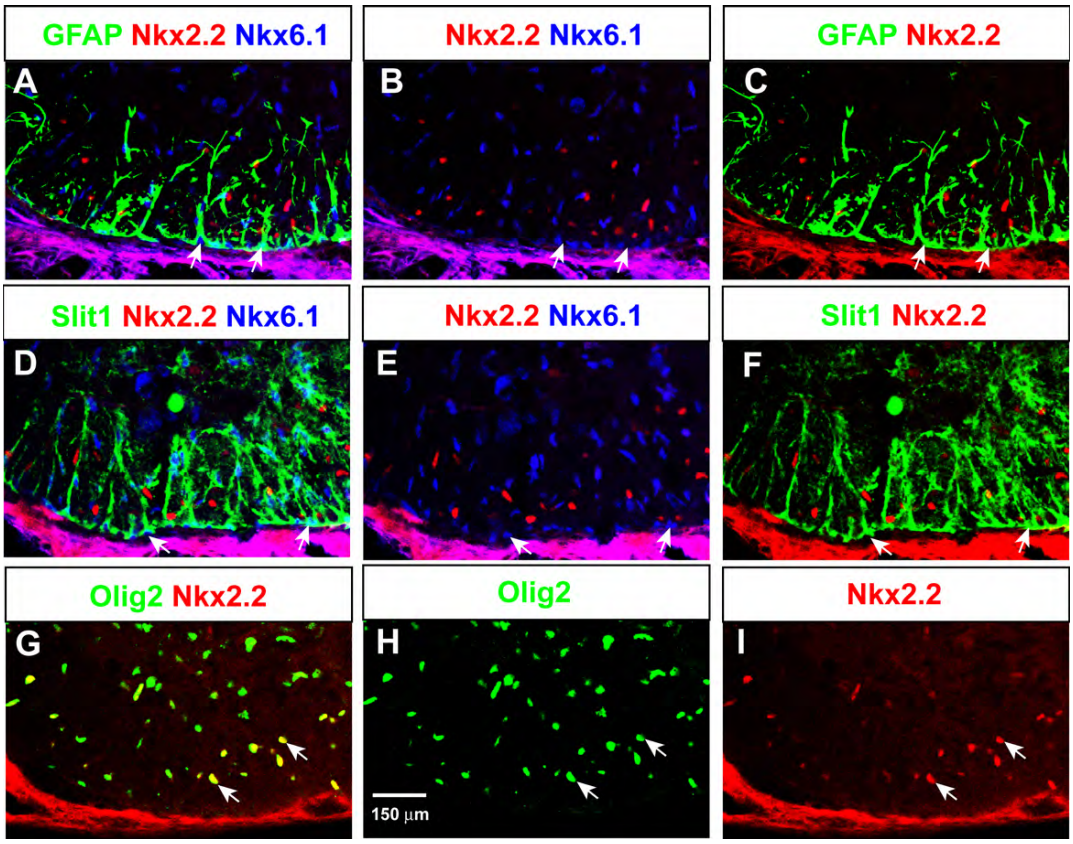

Figure S6. Nkx2.2 is not expressed in VA3 astrocytes

Sections through the ventro-medial white matter of murine E18.5 *Slit1-GFP/+* embryos, double-or triple-labeled with the indicated antibodies. (A-C) Most Nkx6.1^{+} GFAP^{+} VA3 astrocytes (A, arrows) are Nkx2.2^{-} (B, C, arrows), as are Nkx6.1^{+} Slit1^{+} astrocytes (E, F, arrows). By contrast, the majority of Nkx2.2^{+} cells in the white matter at this stage co-express Olig2 (G-I, arrows), indicating that they are oligodendrocyte precursors (Qi et al., 2001; Zhou et al., 2001).

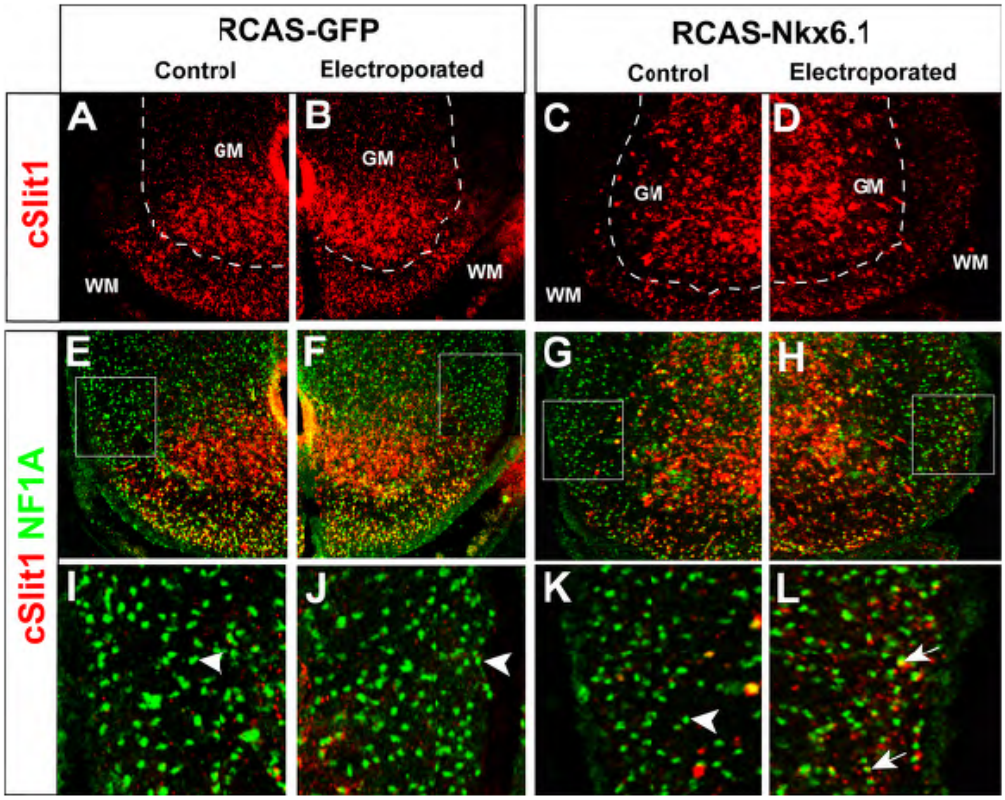

Figure S7. Nkx6.1 is sufficient to promote astrocytic Slit1 expression in lumbar spinal cord

Sections from E12 chick spinal cord of embryos electroporated with a control RCAS-GFP (A-B, E-F, I-J) or RCAS-Nkx6.1 (C-D, G-H, K-L) construct, double-labeled with antibodies to NF1A and a cSlit1 in situ hybridization probe. Panels (E-H) are the same as (A-D), but include the NF1A channel. Panels (I-L) represent higher magnification views of the boxed areas shown in panels (E-H), respectively. Arrows in (L) indicate ectopic expression of cSlit1 in dorso-lateral (presumptive VA1) astrocytes. The induction of astrocytic cSlit1 by Nkx6.1 at this caudal axial level makes it unlikely that this phenotype is secondary to effects of Nkx6.1 to promote V2 IN formation at the expense of V0/V1 IN formation (Briscoe et al., 2000; Vallstedt et al., 2001), because these IN phenotypes are seen only at more anterior axial levels in gain-of-function experiments (Briscoe et al., 2000). Furthermore, direct analysis of V1 INs at E5 showed no changes at axial levels where Nkx6.1 clearly promoted increased Slit1 expression in the VZ (see Supplemental Figure S5).

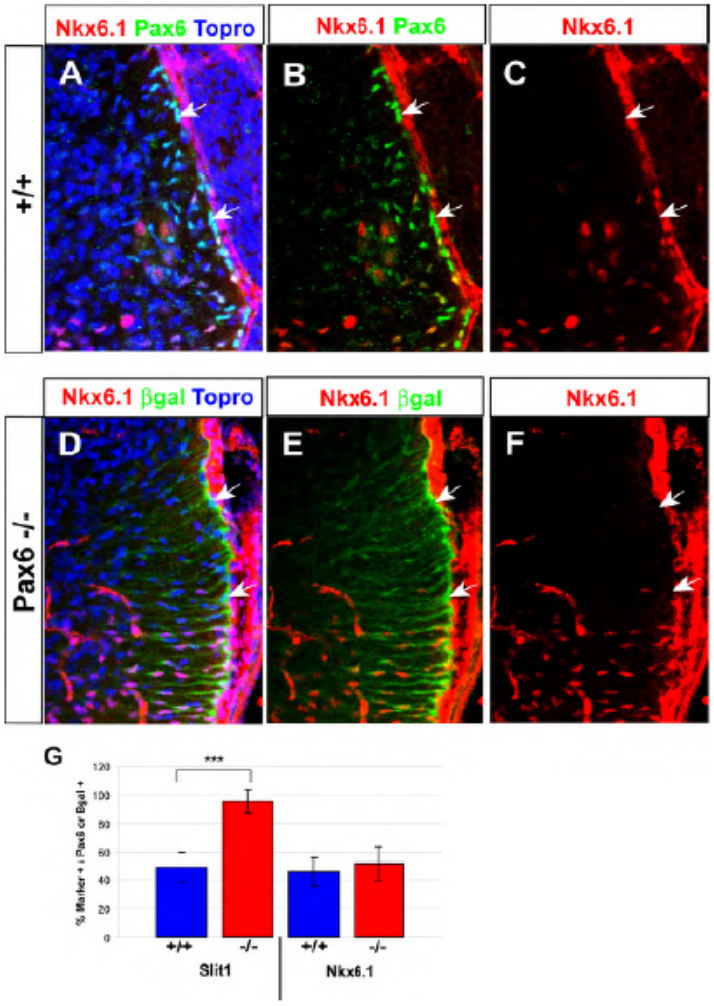

Figure S8. Nkx6.1 is not de-repressed in VA1 astrocytes in *Pax6*$^{-/-}$ embryos

Sections of E18.5 mouse spinal cord from wild-type (A-C) or *Pax6*$^{lacZ/lacZ}$ (D-F) embryos, double labeled for Nkx6.1 and either Pax6 (A-C) or ßgal (D-F). Arrows in (A-C) indicate Pax6^{+} Nkx6.1^{-} VA1 astrocytes. In the *Pax6*$^{lacZ/lacZ}$ mutants, ßgal is used as a surrogate for Pax6 expression (D-F). Note that there is no de-repression of Nkx6.1 in the dorsal ßgal^{+} cells in the mutant (E, F, arrows). (G) quantification confirms that de-repression of Slit1 in Pax6-expressing VA1 astrocytes is not accompanied by de-repression of Nkx6.1.

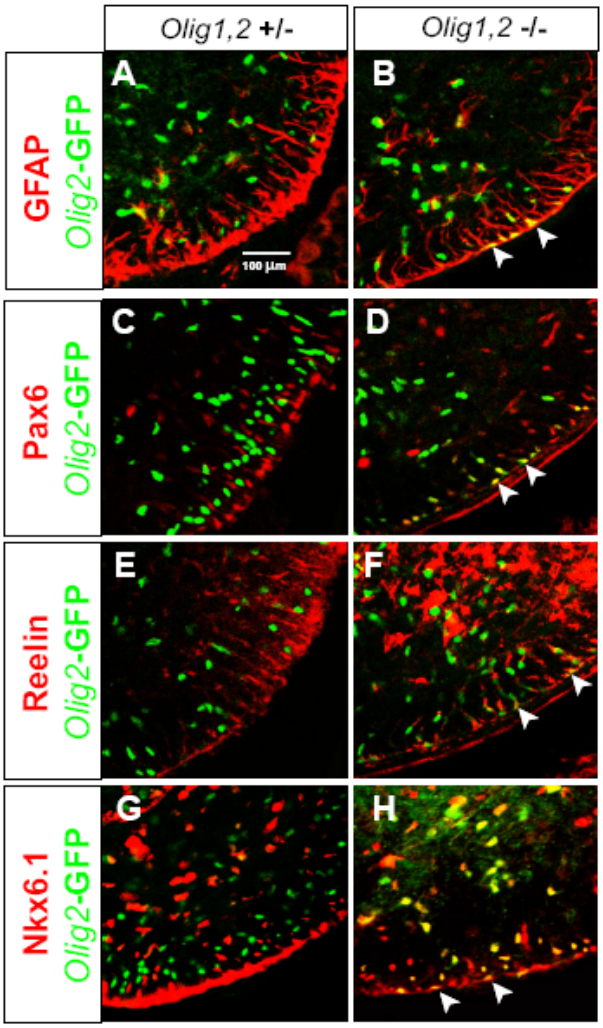

Figure S9. *Olig2*-expressing oligodendrocytes are converted to VA2 astrocytes in the absence of Olig2 function.

Panels illustrate sections through the E18.5 spinal cord white matter of *Olig2-GFP* heterozygous (A, C, E, G) or homozygous (B, D, F, H) embryos, counter-stained with the indicated markers (red). The GFP serves as a lineage tracer to mark the fate of *Olig2*-expressing cells in *Olig2*$^{-/-}$ mutants. In the absence of Olig2, presumptive oligodendrocyte precursors are converted to GFAP^{+} WMAs (A, B), as demonstrated previously (Zhou and Anderson, 2002). These WMAs express Pax6, Reelin and Nkx6.1 (C-H), suggesting that they are VA2 astrocytes. (It was not possible to stain for Slit1, because Slit1 visualization requires a Slit1-GFP knockin reporter, which cannot easily be distinguished from Olig2-GFP.)